Characterization of the nonlinear electrophoretic behavior of colloidal particles in a microfluidic channel

Adrian Lomeli-Martin[†], Olivia D. Ernst[†], Braulio Cardenas-Benitez[§], Richard Cobos[‡], Aditya S. Khair[‡], and Blanca H. Lapizco-Encinas[†,*]

[†] Microscale Bioseparations Laboratory and Biomedical Engineering Department, Rochester Institute of Technology, 160 Lomb Memorial Drive, Rochester, New York, 14623, United States.

[§] Department of Biomedical Engineering, University of California, Irvine, Irvine, CA 92697, USA;

[‡] Department of Chemical Engineering, Carnegie Mellon University, 5000 Forbes Ave, Pittsburgh, Pennsylvania, 15213, United States.

Blanca H. Lapizco-Encinas (PhD)
Email: bhlbme@rit.edu

ABSTRACT

Contemporary findings in the field of insulator-based electrokinetics have demonstrated that in systems under the influence of DC fields, DEP is not the main electrokinetic mechanism responsible for particle manipulation, but rather the sum of electroosmosis, linear and nonlinear electrophoresis. Recent microfluidic studies have brought forth a methodology capable of experimentally estimating the nonlinear electrophoretic mobility of colloidal particles. This methodology, however, is limited to particles that fit two conditions: (i) the particle charge has the same sign as the channel wall charge and, (ii) the magnitude of the particle zeta potential is lower than that of the channel wall. The present work aims to expand upon this methodology by including particles whose zeta potential has a magnitude larger than that of the wall, referred to as "type 2" particles, as well as to report findings on particles that appear to still be under the influence of the linear electrophoretic regime even at extremely high electric fields (~6000 V/cm), referred to as "type 3" particles. Our findings suggest that both particle size and charge are key parameters in the determination of nonlinear electrophoretic properties. Type 2 microparticles were all found to be small (diameter ~ 1 μm) and highly charged, with zeta potentials above -60 mV; in contrast, type 3 microparticles were all large with zeta potentials between -40 and -50 mV. However, it was also hypothesized that other, non-considered parameters could be influencing the results, especially at higher electric fields (> 3000 V/cm). The present work also aims to identify the current limitations in the experimental determination of $\boldsymbol{\mu_{EP,NL}}$ and propose a framework for future work to address the current gaps in the evolving topic of nonlinear electrophoresis of colloidal particles.

Keywords:
Colloidal particles
Electrokinetics
Electroosmosis
Electrophoresis
Microfluidics
Microparticles

Bioanalysis in microfluidic devices is a field where new and exciting discoveries are constantly being made, both theoretically and experimentally.[1–4] There is significant interest in the development of fast separation methods for bioparticles of interest, ranging from macromolecules to microorganisms. Several reliable methods exist for the swift assessment and analysis of nano-sized particles such as DNA and proteins. These methods include, but are not limited to, chromatography and capillary electrophoresis. However, similar efficient techniques have not been developed for the rapid analysis of micron-sized colloidal particles, such as microorganisms.[5,6] Electrokinetics (EK) offers a great potential for the development of rapid label-free separation methods of micron-sized particles, as EK only depends on the physical properties of the particles and offers highly discriminatory separation capabilities.[7] Employing EK allows combining several phenomena within the same microdevices; the most common EK phenomena utilized for rapid separation and assessment of bioparticles of interest are electrophoresis (EP), electroosmosis (EO), dielectrophoresis (DEP) and electrorotation (EROT).[6,8,9]

Recent developments in the field of insulator-based electrokinetics (iEK) by Rouhi et al.,[10] Tottori et al.,[11] Bentor et al.,[12] and Cardenas Benitez et al.;[13] illustrated the importance of the EK phenomenon of nonlinear EP, also called EP of the second kind. Experimental observations of nonlinear EP were first reported in 1972.[14] Numerous mathematical models have been developed to describe the migration of colloidal particles under the effects of nonlinear EP. However, the last few decades have seen a significant surge on studies focusing on nonlinear EP[15]. Several research groups in the field of physics and colloidal science have recently described the distinct regimes of nonlinear EP, to name a few, the contributions by Baran,[16] Dukhin,[17–19] Khair,[20] Mishchuk and Barinova,[21,22] Schnitzer and Yariv,[23–25] and Shilov;[26] have advanced the understanding of nonlinear EP.

Three recent reports illustrating the effect of nonlinear EP in iEK systems[10–13] have transformed the understanding of the migration of colloidal particles in the field of iEK and resulted in a new approach for designing iEK separation processes that includes the effect of nonlinear EP.[27] These recent reports[10–13] unveiled that in systems under the influence of DC fields, DEP is not the main electrokinetic mechanism responsible for particle manipulation, but rather the sum of electroosmosis, linear and nonlinear electrophoresis. Furthermore, the work by Cardenas-Benitez et al.[13] also defined a new EK parameter identified as the electrokinetic equilibrium condition (E_{EEC}), which defines the electric field magnitude at which the overall particle velocity is zero, *i.e.*, all EK phenomena exerted on the particle are in equilibrium ($\mathbf{v}_{EO} + \mathbf{v}_{EP,L} + \mathbf{v}_{EP,NL} = 0$). Once the E_{EEC} value of a particle has been experimentally determined, it is then possible to estimate the mobility of the nonlinear EP velocity of the particle, if this velocity is assumed to have a cubic dependence with the electric field, which is indeed the predicted dependence under certain regimes of nonlinear EP. However, this methodology only works if the particle fulfills the following conditions (i) the particle charge has the same sign of the channel wall charge and, (ii) the magnitude of the particle zeta potential is lower than that of the channel wall. In two recent reports on the characterization of mobility of nonlinear EP[13,28] the microchannels employed had a negative wall zeta potential and all particles had negative particle zeta potentials that were lower in magnitude than that of the channel wall. These statements also hold true for the work reported by Bentor et al.,[12] and Ernst et al.,[29] where the authors experimentally determined the mobility of the nonlinear EP velocity for latex microparticles of varying sizes and surface charge values, all of which had negative zeta potentials with magnitudes lesser than that of the channel wall.

There is no established methodology yet for the nonlinear EP velocity characterization of particles whose zeta potential has a greater magnitude than that of the channel wall or for the particles with opposite charge than the channel wall. The present report describes a methodology for the characterization of microparticles, classified as type 1, type 2, and type 3 (**Figures 1a-1b**). This classification is based on the relation between the particle zeta

potential and the zeta potential of the microchannel wall. The present study employed channels made from polydimethylsiloxane (PDMS), which have a negative wall zeta potential (ζ_W) of -60.1 ± 3.7 mV while employing the suspending medium utilized in this work. Type 1 particles are those that have an electrical charge of the same sign as the channel wall, and their particle zeta potential magnitude is lower than that of the channel wall ($|\zeta_P| < |\zeta_W|$), for these particles, the characterization method has already been developed and reported in the literature[13,28] and is included in this work merely for the sake of completion. The novel aspect of this report pertains to the characterization of the $\mu_{EP,NL}$ of particles labelled as type 2 and type 3. Type 2 particles are those with a particle zeta potential of the same sign of that of the channel wall, but of a greater magnitude ($|\zeta_P| > |\zeta_W|$). Since $\zeta_W = -60.1 \pm 3.7$ mV, all type 2 particles have a negative zeta potential with magnitude greater than 60.1 mV. Type 3 particles, which were initially thought to have a positive particle zeta potential, the opposite sign to that of the channel wall; were found to have a negative charge and exhibit low magnitude of nonlinear EP effects, thereby "delaying" the appearance of nonlinear EP impact in their overall particle velocity. This particular and unexpected behavior of type 3 particles is discussed in detail in the results section. This work is the first report on the characterization of microparticles that are type 2 and type 3 and it complements the previous studies[13,28] that only characterized particles of type 1. The present study is also the first report on the characterization of the nonlinear EP velocity for two distinct dependencies on the electric field strength ($\mathbf{E^3}$ and $\mathbf{E^{3/2}}$) of the three distinct types of particles. The findings presented in this work are expected to be useful in the design of new iEK-based studies, which would expand the fields of bioseparations and bioanalysis by advancing the characterization and separation of microparticles and microorganisms in microfluidic devices.

THEORY

The overall velocity of the migration of microparticles in iEK systems is described by linear and nonlinear EK phenomena. The phenomena that have a linear dependence on the electric field are linear EP and EO. The mobility and velocity expressions for these two linear phenomena, as defined by Helmholtz-Smoluchowski theory, are:

$$\mu_{EP,L} = \frac{\varepsilon_m \zeta_P}{\eta} \quad (1)$$

$$\mathbf{v}_{EP,L} = \mu_{EP,L}\mathbf{E} \quad (2)$$

$$\mu_{EO} = -\frac{\varepsilon_m \zeta_W}{\eta} \quad (3)$$

$$\mathbf{v}_{EO} = \mu_{EO}\mathbf{E} \quad (4)$$

where $\mu_{EP,L}$ represents the linear electrophoretic mobility, μ_{EO} represents the electroosmotic mobility, ε_m and η are the electric permittivity and viscosity of the suspending medium, respectively; $\mathbf{E}$ is the applied electric field, ζ_P and ζ_W represent the zeta potential of the particle and the channel wall, respectively. The particle zeta potential is

employed as a surrogate of the surface charge density of the particle (q_s), which can be estimated with the following expression:[30]

$$q_s = -\sqrt{2\varepsilon_m RT \sum_i c_i \left[exp\left(-\frac{z_i\zeta_P}{\varphi}\right) - 1\right]} \quad (5)$$

where R is the universal gas constant, T is temperature of the system, c_i is the concentration of each of the chemical species that form the suspending media, z_i is the valence of each of these species, and φ is the thermal voltage.

In the linear regime, also known as weak field regime, the linear EP mobility ($\mu_{EP,L}$) is independent of the electric field. The nonlinear EK phenomenon considered in this study is nonlinear EP. In contrast with linear EP, the mobility of nonlinear EP ($\mu_{EP,NL}$) does depend on the magnitude of the electric field. There are several models for describing the behavior of the nonlinear EP velocity of a particle. These models rely on several dimensionless parameters, amongst them are the Peclet (*Pe*) and Dukhin (*Du*) numbers, and the dimensionless field strength β. The *Pe* number is the ratio of the convective to the diffusive movement of the ions located close to surface of the particle. The *Du* number refers to the ratio of the surface conductivity (K^σ) to the bulk conductivity of the medium (K^m). Finally, β is the ratio of the applied electric field magnitude multiplied by the particle radius (a) to the thermal voltage, which has a value is around $25\ mV$ at $298\ K$. Using these parameters, asymptotic expressions for nonlinear electrophoresis have been developed in the case of thin Debye layers.[23–25] The expressions for these three dimensionless parameters are listed below:[22]

$$Pe = \frac{a|v_{EP}|}{D} \quad (6)$$

$$Du = \frac{K^\sigma}{K_m a} \quad (7)$$

$$\beta = \frac{|\mathrm{E}|a}{\varphi} \quad (8)$$

where v_{EP} represents the EP velocity of the particle and D is the diffusion coefficient of the electrolyte ions. Different expressions have been developed to estimate the Du depending on systems' conditions and field of application, the expressions used in this study are included in the supplementary material as **Eqns. (S1-S2)**.

Outside the weak field regime, the EP velocity is no longer linear with the electric field, and the dependence of the EP velocity with the electric field varies with the system conditions as represented by the values of the *Pe* and *Du* numbers. Analytical expressions describing the limiting cases of small *Pe* (*Pe* << 1) and high *Pe* (*Pe* >> 1) values have been developed to determine the dependence of $\mathbf{v}_{EP,NL}$ with the electric field. No analytical expressions exist yet to determine this dependence for intermediate values of *Pe*. The expressions for these two limiting cases illustrating the dependencies of $\mathbf{v}_{EP,NL}$ with the electric field are:[10,24]

$$\mathbf{v}_{EP,NL}^{(3)} = \mu_{EP,NL}^{(3)}\mathbf{E^3} \qquad \text{for } \beta \leq 1,\ Pe << 1 \text{ and arbitrary } Du \quad (9)$$

$$\mathbf{v}_{EP,NL}^{(3/2)} = \mu_{EP,NL}^{(3/2)}\mathbf{E^{3/2}} \quad \text{for } Pe >> 1 \text{ and } Du << 1 \tag{10}$$

Note that **Eqns. (9-10),** are valid for "highly charged particles" as defined by Schnitzer & Yariv,[24] where the dimensionless surface charge density is of order of the inverse of the dimensionless Debye length. Furthermore, these equations are valid in the thin double layer limit where the Debye length is much smaller than the particle's radius. In contrast, for moderately charged particles[24] the electrophoretic velocity is predicted to be linear in the field strength even for β of order one. The present work is the first experimental report on the characterization of both $\mu_{EP,NL}^{(3)}$ and $\mu_{EP,NL}^{(3/2)}$. As shown in **Eqns. (9-10),** at small *Pe* values, which occur at low electric field magnitudes, $\mathbf{v}_{EP,NL}$ scales as $\mathbf{E^3}$; in contrast, at high *Pe* values, which occur at increased electric field magnitudes, $\mathbf{v}_{EP,NL}$ scales $\mathbf{E^{3/2}}$.[22,24] The expression for the overall velocity ($\mathbf{v}_P$) of a colloidal particle in the microchannel depicted in **Figure 1c** becomes:

$$\mathbf{v}_P = \mathbf{v}_{EP,L} + \mathbf{v}_{EO} + \mathbf{v}_{EP,NL} = \mu_{EP,L}\mathbf{E} + \mu_{EO}\mathbf{E} + \mu_{EP,NL}^{(n)}\mathbf{E^n} \tag{10}$$

where the dependency of $\mathbf{v}_{EP,NL}$ with **E**, which is either $\mathbf{E^3}$ or $\mathbf{E^{3/2}}$, is represented by *n* as determined by the operating conditions stated in **Eqns. (9-10),** these being β, the *Pe,* and *Du* numbers (see supplementary material **Tables S1-S3**). As depicted in **Figure 1c**, the channel depth is 40 μm, which is 4-40 times larger than the particle diameter (the particles employed in this study range from 1.0-9.7 μm).

EXPERIMENTAL SECTION

Microdevices. Microchannels were fabricated from PDMS (Dow Corning, MI, USA) using conventional soft lithography techniques.[31] All microchannels were 10.16 mm long, 0.88 mm wide, and 40 μm deep (**Fig. 1c)**. An image of the experimental setup employed in this project is included as **Figure S1a**.

Suspending media. Experiments were done using a buffer solution of K_2HPO_4 with a concentration of 0.2 mM, with the addition of 0.05% (V/V) of Tween 20 to prevent particle adhesion. This suspending media had a conductivity of 40.7 ± 4.0 μS/cm and a pH of 7.3 ± 0.2, which resulted in a wall zeta potential (ζ_W) of -60.1 ± 3.7 mV and μ_{EO} of 4.7 $\pm$ 0.3 $x\ 10^{-8} m^2 V^{-1} s^{-1}$ in the PDMS microchannels. as determined via current monitoring experiments.[32]

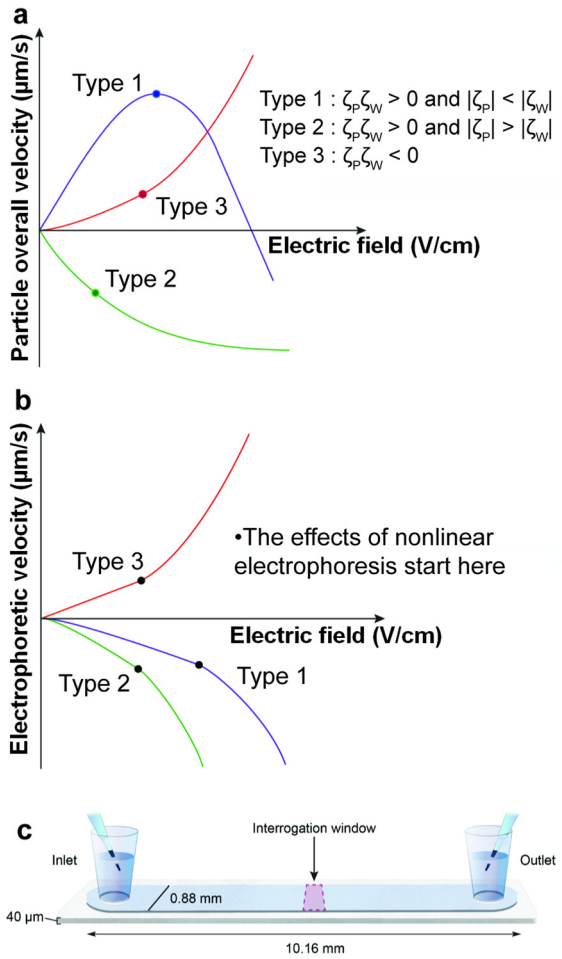

Figure 1. (a) Schematic representation of the particle overall velocity for particles type 1, type 2, and type 3 as a function of the electric field, illustrating the change in the velocity behavior caused by the initiation of nonlinear EP effects. The division between particles is explained as a relation between the zeta potential of the particle (ζ_P) and that of the wall (ζ_W). This represents a system in which $\zeta_W < 0$. **(b)** Schematic representation of the expected particle EP velocity as a function of the electric field for arbitrary type 1, type 2 and type 3 particles. **(c)** Schematics of the microchannel employed for particle tracking velocimetry assessments (Figure S1a contains a picture of the actual experimental setup).

Microparticles. A total of twelve distinct samples of polystyrene microparticles of varying sizes (Magsphere Pasadena, CA, USA and ThermoFisher Scientific Waltham, MA, USA) were studied, and their properties are found summarized in **Table 1**. Samples of microsphere suspensions were prepared by first diluting the concentrated stock solution into the suspending media to a desired microparticle concentration (**Table S4**). Each concentration was empirically determined to allow for the best visualization of the particle migration.

Table 1.

Characteristics of the polystyrene microparticles used in this study.

Particle ID	Diam. (μm)	ζ_P (mV)	Charge/mass x 10^{-3} (C/g)	$\mu_{EP,L}$ x 10^{-8} ($m^2V^{-1}s^{-1}$)	E for $\mu_{EP,NL}^{(3)}$ estimation (V/cm)	$\mu_{EP,NL}^{(3)}$ x 10^{-18} ($m^4V^{-3}s^{-1}$)	E for $\mu_{EP}^{(3/2)}$ estimation (V/cm)	$\mu_{EP,NL}^{(3/2)}$ x 10^{-12} ($m^{5/2}V^{-3/2}s^{-1}$)

Type 1 particles								
Particle 1 (P1)	2.0	-18.9 ± 6.1	-2.7 ± 0.9	-1.5 ± 0.0	500 ± 100	-6.8 ± 0.4	2100 ± 100	-77.9 ± 6.1
Particle 2 (P2)	2.0	-19.2 ± 0.6	-1.6 ± 0.1	-0.9 ± 0.0	400 ± 100	-5.3 ± 0.4	3300 ± 100	-81.7 ± 3.0
Particle 3 (P3)	3.0	-28.2 ± 11.4	-2.7 ± 1.2	-2.2 ± 0.9	350 ± 50	-4.4 ± 2.0	3100 ± 100	-57.7 ± 0.1
Particle 4 (P4)	5.1	-31.4 ± 0.4	-1.7 ± 0.0	-2.4 ± 0.0	200 ± 50	-5.6 ± 1.6	2000 ± 100	-37.9 ± 2.4
Particle 5 (P5)	5.1	-25.5 ± 1.5	-1.5 ± 0.0	-2.1 ± 0.1	200 ± 50	-9.8 ± 2.3	2000 ± 100	-68.4 ± 1.2
Type 2 particles								
Particle 6 (P6)	1.0	-70.9 ± 1.8	-2.5 ± 0.5	-2.4 ± 0.1	500 ± 100	-0.8 ± 0.4	5100 ± 100	-0.5 ± 0.2
Particle 7 (P7)	1.1	-65.6 ± 0.9	-2.0 ± 0.2	-2.9 ± 0.1	500 ± 100	-0.7 ± 0.1	5100 ± 100	-9.9 ± 0.1
Particle 8 (P8)	1.1	-79.4 ± 1.5	- 2.7 ± 0.4	-3.7 ± 0.1	500 ± 100	-0.4 ± 0.1	5100 ± 100	-1.5 ± 0.5
Particle 9 (P9)	1.0	-62.0 ± 0.5	- 2.1 ± 0.1	-3.5 ± 0.3	500 ± 100	-0.4 ± 0.1	5100 ± 100	-11.1 ± 0.2
Type 3 particles								
Particle 10 (P10)	5.0	-43.6 ± 1.6	-2.6 ± 0.0	-3.4 ± 0.1	200 ± 50	-7.3 ± 2.3	3600 ± 100	-6.7 ± 1.1
Particle 11 (P11)	7.6	-47.0 ± 0.8	-1.9 ± 0.0	-3.7 ± 0.0	75 ± 25	-39.4 ± 26.3	3600 ± 100	-1.4 ± 0.8
Particle 12 (P12)	9.7	-22.8 ± 0.5	-1.1 ± 0.0	-3.4 ± 0.0	75 ± 25	-71.2 ± 31.7	3600 ± 100	-1.9 ± 0.5

Equipment and software. The LabSmith *Sequencer* software was utilized to manipulate a high-voltage power supply (Model HVS6000D, LabSmith, Livermore, CA). This unit applied DC voltage sequences to the microchannels via platinum-soldered electrodes. Inverted microscopes were used to record experimental sessions: a Zeiss Axiovert 40 CFL (Carl Zeiss Microscopy, Thornwood, NY) and a Leica Dmi8 (Wetzlar, Germany).

Experimental procedure. Before any experimental runs, the microchannel (shown in **Figure 1c**) was filled with suspending media. The influence of pressure-driven flow was eliminated by adjusting the liquid level at the reservoirs. A 2 μL sample of the selected particle suspension was introduced into the inlet reservoir, then platinum wire electrodes were placed and fixed into both reservoirs. Various DC voltages were applied to assess the effect of the electric field on particle velocity. Increasing electric field values were applied to observe the effects of linear electrophoresis at weak fields, and then the effects of nonlinear electrophoresis at strong fields. Each electric field was applied for a total of 15 seconds and experiments with the same applied electric field were repeated at least four times. The values for ζ_P were estimated employing a methodology described in previous work.[28] In summary, low-voltage particle tracking velocimetry measurements (PTV) were done to determine the values of $\mu_{EP,L}$, and then **Eqn. 1** was employed to estimate ζ_P (**Table 1)**. A screen capture of the software used for the data analysis of the recorded PTV videos is included in the supplementary material as **Figure S1b**.

RESULTS AND DISCUSSION

Characterization of microparticles type 1

A series of PTV experiments were conducted by varying the magnitude of the electric fields (50 to 3200 V/cm) to determine the particle velocity. The results of these experiments are summarized in **Table 1** and **Figure 2**. As noted in **Table 1**, type 1 particles vary in both size and ζ_P. First, low electric fields were employed to

determine $\mu_{EP,L}$ and ζ_P of each particle. Then, higher electric fields (> 150 V/cm) were used to observe particle migration under nonlinear electrophoresis and obtain the $\mu_{EP,NL}$ for two distinct dependencies on the electric field ($\mathbf{E^3}$ and $\mathbf{E^{3/2}}$). This allowed determining $\mu_{EP,NL}^{(3)}$ at lower electric fields and $\mu_{EP,NL}^{(3/2)}$ at higher electric fields, respectively, using comparable values of β (see **Eqn. 8** and **Tables S1-S3**). For type 1 microparticles, the behavior of the overall particle velocity as a function of the electric field was as follows: first a linear increase was observed, then $\mathbf{v}_P$ reached a maximum, and as the electric field kept increasing, $\mathbf{v}_P$ decreased until it turned negative, *i.e*., the particle migration switched direction.

As observed in **Table 1** regarding the results under the weak field regime, the experimentally obtained ζ_P values for the five particles covered in this section varied from -18.9 to -31.4 mV, thus all these particles fit the criteria set for type 1 microparticles ($|\zeta_P| < |\zeta_W|$). The observed $\mathbf{v}_P$ of each type 1 microparticle as a function of the electric field is shown in **Figure 2a,** where all particles followed the behavior in previous studies.[13,28] By analyzing the results under the strong field regime, it is observed in **Table 1** that, with the exception of P1, the magnitude of $\mu_{EP,NL}^{(3)}$ increased[18] while, aside from P2, the magnitude of $\mu_{EP,NL}^{(3/2)}$ exhibited a decrease with particle size.[22] These results appear to be consistent with the work reported by Bentor et al.[12] where a similar trend was observed. Particle charge (in terms of ζ_P) also has an interesting effect on both $\mu_{EP,L}$ and $\mu_{EP,NL}$. Larger magnitudes of ζ_P as expected, resulted in larger magnitudes of $\mu_{EP,L}$, but smaller magnitudes of $\mu_{EP,NL}$ in both regimes. While no work has determined a clear relationship between particle charge and $\mu_{EP,NL}$ yet, O'Brien and White[33] have shown that $\mu_{EP,L}$ does vary with ζ_P in a given suspending medium. As the ζ_P increases, so does the $\mu_{EP,L}$, and after reaching a maximum magnitude, $\mu_{EP,L}$ starts to decrease. They attributed this behavior to retardation forces, due to the Debye cloud, scaling faster with ζ_P than the electrical force on the particle, manifesting as a reduced net electrophoretic mobility. This is caused by surface conduction on the particle, which becomes more prominent in thin Debye layers and large zeta potentials. Although these statements were reported for weak fields, given the experimental results obtained in this work it is possible for them to also hold true for moderate to strong fields.[33]

The electrophoretic velocity of each type 1 microparticle as a function of the electric field is shown in **Figure 2b**. Since all particles exhibited negative EP velocities, the figure shows the absolute value of these velocities for ease of visualization. As expected, the $\mathbf{v}_{EP}$ of type 1 microparticles presented a range of linearity, after which it can be observed that the behavior of $\mathbf{v}_{EP}$ changes slightly, indicating the presence of nonlinear EP effects. P1 and P5 present larger $\mathbf{v}_{EP}$ magnitudes compared to the rest of the type 1 particles, which is consistent with those being the two particles where $\mathbf{v}_P$ changed sign at the smallest applied field strength. These observations seem to be consistent with the experimental results obtained for $\mu_{EP,NL}^{(3)}$, where both particles present the largest magnitudes

in the $\mu_{EP,NL}^{(3)}$ regime amongst the other type 1 microparticles. As shown in **Figure S2** of the supplementary material, both P1 and P5 fail to follow the expected velocity profile corresponding to the $\mathbf{E}^{3/2}$ dependency even at the highest of experimental electric fields, suggesting that the obtained $\mu_{EP,NL}^{(3/2)}$ value might not be entirely representative of the particle's proper behavior at that electric field range.

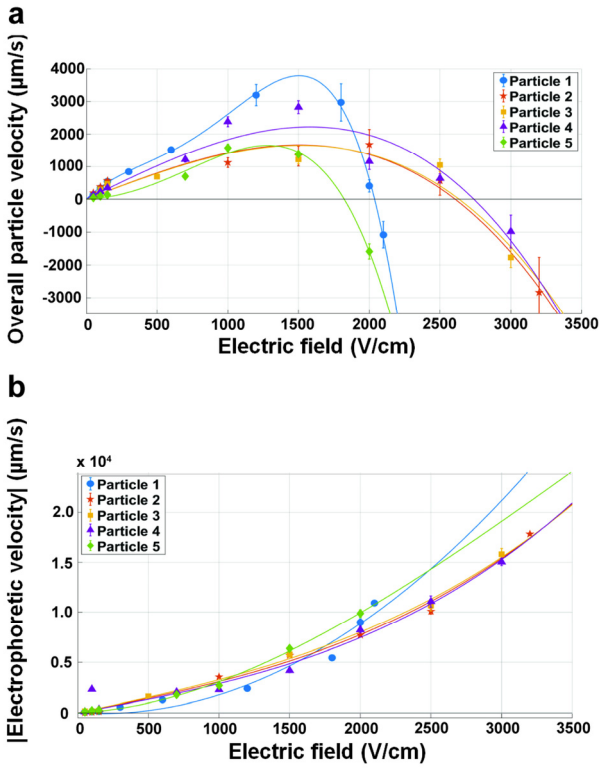

Figure 2. Plots of particle velocity as a function of the electric field for microparticles type 1. **(a)** Overall particle velocity ($\mathbf{v}_P$). (**b)** Absolute value of the particle electrophoretic velocity ($\mathbf{v}_{EP}$). Markers indicate experimental data, and the solid-colored lines are included for ease of visualization. Error bars denote standard deviation.

Characterization of microparticles type 2

After a particle was identified as being type 2 ($|\zeta_P| > |\zeta_W|$) through ζ_P measurements in the weak field regime, additional PTV experiments were done to obtain a full set of $\mathbf{v}_P$ measurements. The results of these experiments are summarized in **Table 1** and **Figure 3**. As shown in **Table 1**, all the particles identified to follow type 2 behavior are small (diameter ~ 1.0 μm) compared to the rest of the particles used in this work. This commonality in size can be attributed to the fact that the absolute value of ζ_P in small particles tends to be greater than that of large particles.[34] Physically smaller particles have a greater surface to volume ratio when compared to larger particles,[35] *i.e.*, since the electrical charge of a particle is on its surface, smaller particles have a higher charge per unit volume. This could explain the common tendency in higher ζ_P magnitude that type 2 microparticles present. The experimentally obtained values for ζ_P of the four particles covered in this section ranged from -62.0 to -79.4 mV.

The observed $\mathbf{v}_P$ of each type 2 microparticle as a function of the electric field is shown in **Figure 3a**, where, as expected, all particles moved with a negative velocity. The magnitude of $\mathbf{v}_P$ in all type 2 microparticles seemed to be directly proportional to the intensity of the electric field. Eventually, all particles showed a slight change in their $\mathbf{v}_P$ behavior, attributed to the presence of nonlinear electrophoretic effects. However, as can be seen in **Figure 3b**, which shows the absolute value of the electrophoretic velocity ($|\mathbf{v}_{EP}|$) of each type 2 microparticle as a function of the electric field, all particles seem to follow an almost linear behavior even at high field strengths. This is supported by the experimentally obtained $\mu_{EP,NL}^{(3)}$ values, which are the smallest out of all the particles in this set of experiments. Considering the potential experimental error, the $\mu_{EP,NL}^{(3)}$ values for P6 and P8 could be due to rounding errors.

Evidence supporting an extended linear behavior, shown in **Figure 3b**, can be also observed in **Figure S3** which illustrates the dimensionless velocity (**Eqns. S5-S6**) as a function of the electric field magnitude, where neither of the nonlinear behaviors properly fits the particles. The only exception is P8 with the $\mathbf{E}^{3/2}$ expression, which is primarily linear in that range of electric field. It is currently unknown if these particles simply cannot enter the nonlinear electrophoretic regime due to their intrinsic properties, or if other forces like electroosmosis of the second kind,[36] could be interfering. Future work will focus on determining this.

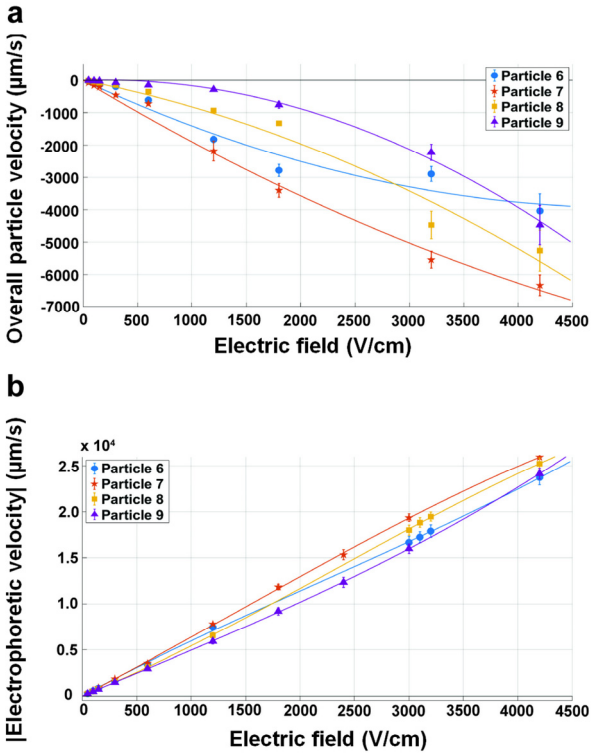

Figure 3. Plots of particle velocity as a function of the electric field for microparticles type 2. **(a)** Overall particle velocity ($\mathbf{v}_P$). (**b)** Absolute value of the particle electrophoretic velocity ($\mathbf{v}_{EP}$). Markers indicate experimental data, and the solid-colored lines are included for ease of visualization. Error bars denote standard deviation.

Characterization of microparticles type 3

Type 3 particles were initially assumed to have a positive charge ($\zeta_P > 0$), thus, were expected to migrate always in the positive direction, *i.e.*, $\mathbf{v}_P$ was expected to keep increasing as a function of the electric field. These particles would never cross the zero-velocity-line ($\mathbf{v}_P = 0$) as type 1 particles did. A particle was deemed to be type 3 if it kept moving with a positive velocity at the highest possible voltage output allowed by our high voltage power supply (6000 V). The results of the characterization experiments of type 3 particle are summarized in **Table 1** and **Figure 4**.

For this section, data analysis was performed until 5500 V/cm since higher electric fields produced $\mathbf{v}_P$ values too high to be accurately measured by our experimental setting. The experimentally obtained ζ_P values of these particles ranged from -25.5 to -47.0 mV. Surprisingly, these do not fit the initial criteria proposed for type 3 particles ($\zeta_P > 0$). Revisions to the initial selection criteria between particles were necessary. It was hypothesized that particles would continue to have positive velocities if they possessed weak $\mu_{EP,NL}$ under nonlinear electrophoresis; in that case, the electroosmotic velocity would always be greater than the electrophoretic velocity in terms of magnitude ($|\mathbf{v}_{EO}| > |\mathbf{v}_{EP}|$).

The observed $\mathbf{v}_P$ of each type 3 microparticle as a function of the electric field is shown in **Figure 4a**. The behavior exhibited by P12 hints to what is happening. The $\mu_{EP,NL}$ value of these particles has a negative sign; therefore, $\mu_{EP,NL}$ should also follow in the same direction as explained by Dukhin.[18] Consequently, we are not dealing with particles that move with positive velocity indefinitely as was initially expected. Instead, these are simply type 1 particles that cross the zero-velocity-line ($\mathbf{v}_P = 0$) outside the experimental boundaries of our setup. This is further confirmed in **Figure 4b**, where P12 exhibits the same trend seen in type 1 microparticles when the nonlinear electrophoretic effects start gaining traction within the system at higher electric fields. Despite their similarities, there is still merit in distinguishing type 3 from type 1 microparticles. In most electrokinetic separation devices,[27,37] the electric field in the system will be in a range under which the effects of nonlinear electrophoresis would be significant for type 1 particles, while almost non-existent for type 3 particles, as type 3 particles have a "delayed" response to nonlinear electrophoresis. This response is consistent with the lower surface charge of these particles in comparison to type 1 particles. For practical purposes, when designing a microparticle separation, there is a clear distinction between type 1 and type 3 particles, where the former would clearly show in their migration the effects of nonlinear electrophoresis, while the latter would not. [27,37] These

observations are not unprecedented; since Kumar et al.[38] reported a linear $\mathbf{v}_{EP}$ of particles even at high fields' strengths. Although the size and surface charge of the particles they employed are different from the ones used in our experiments, these being 4 μm in diameter and moderately charged particles, the reported particle movement indicated the characteristic type 3 behavior.

An interesting observation arises when analyzing the $\mu_{EP,NL}$ values of the identified type 3. The magnitudes of $\mu_{EP,NL}^{(3)}$ are amongst the largest of the particles in this project, which given their size, is consistent with what has been reported in previous literature.[18] However, this would imply that these particles quickly transition into moving with negative velocity, as seen when analyzing type one particles, which did not occur. This could be due to the $\mathbf{E}^3$ expression not being representative of type 3 particle behavior. Type 3 particles possess the smallest average $\mu_{EP,NL}^{(3/2)}$ values in this project, which would explain why they failed to adopt negative velocity values once leaving the weak field regime. Additionally, as shown in **Figure S4**, the $\mathbf{E}^{3/2}$ expression seemed to be a better fit for these particles. This provides a possible explanation as to why the deviation in $\mu_{EP,NL}^{(3/2)}$ values are noticeably smaller than the $\mu_{EP,NL}^{(3)}$ ones. Both particle size and particle charge seem to be determining factors in the electromigration behavior of the microparticles. All three of the type 3 microparticles identified in this work share some commonalities: (i) they are large (5.0-9.7 μm in diameter), and (ii) they present the same surface functionalization (carboxylated). Further studies are needed to verify if these factors, or any possible interaction between them, are what makes type 3 particles exhibit a delayed or weak nonlinear EP behavior.

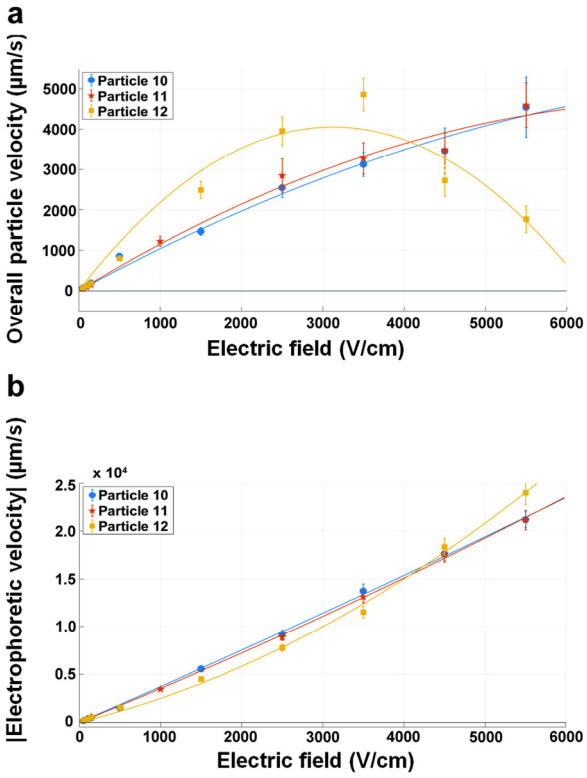

Figure 4. Plots of particle velocity as a function of the electric field for microparticles type 3. **(a)** Overall particle velocity ($\mathbf{v}_P$). (**b)** Absolute value of the particle electrophoretic velocity ($\mathbf{v}_{EP}$). Markers indicate experimental data, and the solid-colored lines are included for ease of visualization. Error bars denote standard deviation.

CONCLUSIONS

In this study, particles were divided into three distinct categories according to the direction of their velocity when subjected to strong DC electric fields. These categories are summarized in **Figure 5**. Particles identified as "type 1," for which $|\zeta_P| < |\zeta_W|$, possessed a range of positive velocity which decreased and then reversed once a threshold, coined the E_{EEC} (which occurs when the particle crosses the zero-velocity-line, $\mathbf{v}_P = 0$), was reached. Although some of the results for this particle type appeared consistent with what is reported in the literature, the observed deviations could be interpreted as an indication of the importance that other parameters or phenomena not currently being considered may have on the system, such as EO of the second kind. "Type 2" particles, for which $|\zeta_P| > |\zeta_W|$, start off having negative velocity due to their $\mu_{EP,L}$ values already being greater than the μ_{EO} of the fluid in magnitude. A commonality shared between all the particles identified as type 2 is their size. Smaller particles have greater absolute values of particle zeta potential than those of larger particles, attributed to a greater surface charge to volume ratio, as charge is on the particle surface. Type 2 particles exhibited $\mu_{EP,NL}$ values so small that they could be attributed to rounding errors, resulting in an almost linear $\mathbf{v}_{EP,NL}$ behavior. Future work will seek to explain why these particles exhibit an extended region of linear behavior. "Type 3" particles, which

were initially thought as having a positive ζ_P, are those that despite of their negative surface charge (thus, negative ζ_P), still show a positive overall velocity even at the high (6000 V/cm) experimental limit of the employed instruments. Some commonalities between these particles imply that size, surface functionalization, and electrical charge could be determining factors in the behavior adopted by microparticles once subjected to electric fields. Future work will focus on confirming these observations and finding concrete discerning characteristics between type 3 and type 1 microparticles. The field of experimental characterization of the mobility of the nonlinear electrophoretic velocity is constantly evolving, and our understanding of the different factors and phenomena at play in these systems also is still developing. Given that the effects of nonlinear electrophoresis are essential for the selection of appropriate conditions for successful EK-based separations, the findings presented here will be used for the design of new iEK-based assessments and separations of microparticles and cells. Further insight in type 2 and type 3 particle behavior would expand the possible options for the separation of particles that do not fit the separation criteria set by type 1 particles. This, in turn, would allow novel and exciting iEK-based separations that would advance the field of microfluidic bioanalysis.

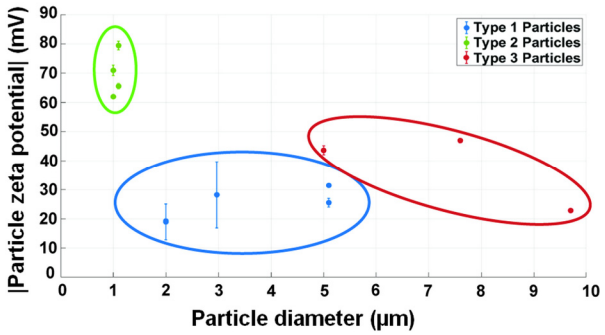

Figure 5. Scatter plot of the absolute value of the negative particle zeta potentials as a function of particle diameter for all twelve particles in this work. Each type of microparticle is represented by a different color: blue (type 1), green (type 2), and red (type 3). Error bars denote standard deviation.

ASSOCIATED CONTENT

Supporting Information

The supporting information file contains a file with the parameters used to assess the electric field dependency for each of the defined regimes (Tables S1-S3), particle concentration used for experiments (Table S4), the experimental setup employed in the project along with a screen capture of the software used for data analysis (Figure S1), and how each of the particle's velocity fit with the E^3 and $E^{3/2}$ expressions (Figures S2-S4).

AUTHOR INFORMATION

Corresponding Author

Email: bhlbme@rit.edu

ORCID

Adrian Lomeli-Martin: 0000-0003-2215-3449

Olivia D. Ernst: 0000-0003-1828-6724

Braulio Cardenas-Benitez: 0000-0002-8259-3705

Richard Cobos: 0000-0002-6035-6370

Aditya S. Khair: 0000-0001-6076-2910

Blanca H. Lapizco-Encinas: 0000-0001-6283-8210

Author contributions

ALM: Experimentation, Data Analysis, Writing Original Draft – Review & Editing. **ODE**: Experimentation, Data Analysis, Review of the Paper. **BCB**: Methodology, Data Analysis, Review & Editing. **RCF**: Methodology, Data Analysis, Review & Editing. **AK**: Methodology, Data Analysis, Review & Editing. **BHLE**: Conceptualization, Methodology, Project Administration, Supervision, Writing Original Draft – Review & Editing.

Notes:

The authors declare that they have no known competing financial interest or personal relationships that could have appeared to influence the work reported in this paper.

ACKNOWLEDGEMENTS

This material is based upon work supported by the National Science Foundation under Award No. 2127592 and No. 2002120. The authors would like to thank Joanne Park for her assistance in the elaboration of Figure 1 of this manuscript.

REFERENCES

(1) Liu, W.; Ren, Y.; Tao, Y.; Chen, X.; Yao, B.; Hui, M.; Bai, L. Control of Two-Phase Flow in Microfluidics Using out-of-Phase Electroconvective Streaming. *Phys. Fluids* **2017**, *29* (11). https://doi.org/10.1063/1.5003973.

(2) Liu, W.; Ren, Y.; Tao, Y.; Yao, B.; Liu, N.; Wu, Q. A Universal Design of Field-Effect-Tunable Microfluidic Ion Diode Based on a Gating Cation-Exchange Nanoporous Membrane. *Phys. Fluids* **2017**, *29* (11). https://doi.org/10.1063/1.5001051.

(3) Csala, H.; Dawson, S. T. M.; Arzani, A. Comparing Different Nonlinear Dimensionality Reduction Techniques for Data-Driven Unsteady Fluid Flow Modeling. *Phys. Fluids* **2022**, *34* (11). https://doi.org/10.1063/5.0127284.

(4) Dahal, E.; Ghammraoui, B.; Badano, A. Characterization of Materials Embedded in Thick Objects Using Spectral Small-Angle X-Ray Scattering. *J. Phys. D. Appl. Phys.* **2020**, *53* (24). https://doi.org/10.1088/1361-6463/ab8248.

(5) Vaghef-Koodehi, A.; Lapizco-Encinas, B. H. Microscale Electrokinetic-Based Analysis of Intact Cells and Viruses. *Electrophoresis* **2022**, *43* (1–2), 263–287. https://doi.org/10.1002/elps.202100254.
(6) Sonker, M.; Kim, D.; Egatz-Gomez, A.; Ros, A. Separation Phenomena in Tailored Micro- and Nanofluidic Environments. *Annu. Rev. Anal. Chem.* **2019**, *12* (1), 475–500. https://doi.org/10.1146/annurev-anchem-061417-125758.
(7) Liu, Y.; Hayes, M. A. Differential Biophysical Behaviors of Closely Related Strains of Salmonella. *Front. Microbiol.* **2020**, *11*, 302. https://doi.org/10.3389/FMICB.2020.00302.
(8) Lapizco-Encinas, B. H. The Latest Advances on Nonlinear Insulator-Based Electrokinetic Microsystems under Direct Current and Low-Frequency Alternating Current Fields: A Review. *Analytical and Bioanalytical Chemistry*. Springer October 19, 2022, pp 885–905. https://doi.org/10.1007/s00216-021-03687-9.
(9) Liang, W.; Yang, X.; Wang, J.; Wang, Y.; Yang, W.; Liu, L. Determination of Dielectric Properties of Cells Using AC Electrokinetic-Based Microfluidic Platform: A Review of Recent Advances. *Micromachines* **2020**, *11* (5), 513. https://doi.org/10.3390/mi11050513.
(10) Rouhi Youssefi, M.; Diez, F. J. Ultrafast Electrokinetics. *Electrophoresis* **2016**, *37* (5–6), 692–698. https://doi.org/10.1002/elps.201500392.
(11) Tottori, S.; Misiunas, K.; Keyser, U. F.; Bonthuis, D. J. Nonlinear Electrophoresis of Highly Charged Nonpolarizable Particles. *Phys. Rev. Lett.* **2019**, *123* (1), 14502. https://doi.org/10.1103/PhysRevLett.123.014502.
(12) Bentor, J.; Dort, H.; Chitrao, R. A.; Zhang, Y.; Xuan, X. Nonlinear Electrophoresis of Dielectric Particles in Newtonian Fluids. *Electrophoresis* **2022**, *In press.* (November), 1–9. https://doi.org/10.1002/elps.202200213.
(13) Cardenas-Benitez, B.; Jind, B.; Gallo-Villanueva, R. C.; Martinez-Chapa, S. O.; Lapizco-Encinas, B. H.; Perez-Gonzalez, V. H. Direct Current Electrokinetic Particle Trapping in Insulator-Based Microfluidics: Theory and Experiments. *Anal. Chem.* **2020**, *92* (19), 12871–12879. https://doi.org/10.1021/acs.analchem.0c01303.
(14) Dukhin, A. S.; Dukhin, S. S. Aperiodic Capillary Electrophoresis Method Using an Alternating Current Electric Field for Separation of Macromolecules. *Electrophoresis* **2005**, *26* (11), 2149–2153. https://doi.org/10.1002/elps.200410408.
(15) Khair, A. S. Nonlinear Electrophoresis of Colloidal Particles. *Current Opinion in Colloid and Interface Science*. Elsevier March 25, 2022, p 101587. https://doi.org/10.1016/j.cocis.2022.101587.
(16) Barany, S. Electrophoresis in Strong Electric Fields. *Advances in Colloid and Interface Science*. Elsevier March 1, 2009, pp 36–43. https://doi.org/10.1016/j.cis.2008.10.006.
(17) Dukhin, A. S.; Ulberg, Z. R.; Gruzina, T. G.; Karamushka, V. I. Peculiarities of Live Cells' Interaction with Micro- and Nanoparticles. In *Colloid and Interface Science in Pharmaceutical Research and Development*; Elsevier Inc., 2014; pp 193–222. https://doi.org/10.1016/B978-0-444-62614-1.00010-7.
(18) Dukhin, S. S. Electrokinetic Phenomena of the Second Kind and Their Applications. *Adv. Colloid Interface Sci.* **1991**, *35* (C), 173–196. https://doi.org/10.1016/0001-8686(91)80022-C.
(19) Dukhin, S. S. Non-Equilibrium Electric Surface Phenomena. *Adv. Colloid Interface Sci.* **1993**, *44* (C), 1–134. https://doi.org/10.1016/0001-8686(93)80021-3.
(20) Khair, A. S. Strong Deformation of the Thick Electric Double Layer around a Charged Particle during Sedimentation or Electrophoresis. *Langmuir* **2018**, *34* (3), 876–885. https://doi.org/10.1021/acs.langmuir.7b01897.
(21) Mishchuk, N. A. Concentration Polarization of Interface and Non-Linear Electrokinetic Phenomena. *Advances in Colloid and Interface Science*. Elsevier B.V. October 15, 2010, pp 16–39. https://doi.org/10.1016/j.cis.2010.07.001.
(22) Mishchuk, N. A.; Barinova, N. O. Theoretical and Experimental Study of Nonlinear Electrophoresis. *Colloid J.* **2011**, *73* (1), 88–96. https://doi.org/10.1134/S1061933X11010133.
(23) Schnitzer, O.; Zeyde, R.; Yavneh, I.; Yariv, E. Weakly Nonlinear Electrophoresis of a Highly Charged Colloidal Particle. *Phys. Fluids* **2013**, *25* (5), 052004. https://doi.org/10.1063/1.4804672.
(24) Schnitzer, O.; Yariv, E. Nonlinear Electrophoresis at Arbitrary Field Strengths: Small-Dukhin-Number

Analysis. *Phys. Fluids* **2014**, *26* (12), 122002. https://doi.org/10.1063/1.4902331.
(25) Schnitzer, O.; Yariv, E. Macroscale Description of Electrokinetic Flows at Large Zeta Potentials: Nonlinear Surface Conduction. *Phys. Rev. E* **2012**, *86* (2), 021503. https://doi.org/10.1103/PhysRevE.86.021503.
(26) Shilov, V.; Barany, S.; Grosse, C.; Shramko, O. Field-Induced Disturbance of the Double Layer Electro-Neutrality and Non-Linear Electrophoresis. *Adv. Colloid Interface Sci.* **2003**, *104* (1–3), 159–173. https://doi.org/10.1016/S0001-8686(03)00040-X.
(27) Vaghef-Koodehi, A.; Dillis, C.; Lapizco-Encinas, B. H. High-Resolution Charge-Based Electrokinetic Separation of Almost Identical Microparticles. *Anal. Chem.* **2022**, *94* (17), 6451–6456. https://doi.org/10.1021/acs.analchem.2c00355.
(28) Antunez-Vela, S.; Perez-Gonzalez, V. H.; Coll De Peña, A.; Lentz, C. J.; Lapizco-Encinas, B. H. Simultaneous Determination of Linear and Nonlinear Electrophoretic Mobilities of Cells and Microparticles. *Anal. Chem.* **2020**, *92* (22), 14885–14891. https://doi.org/10.1021/acs.analchem.0c03525.
(29) Ernst, O. D.; Vaghef-Koodehi, A.; Dillis, C.; Lomeli-Martin, A.; Lapizco-Encinas, B. H. Dependence of Nonlinear Electrophoresis on Particle Size and Electrical Charge. *Anal. Chem.* **2023**, *In Press*. https://doi.org/10.1021/acs.analchem.2c05595.
(30) Lyklema, J. Electric Double Layers. In *Fundamentals of Interface and Colloid Science*; Academic Press, 1995; Vol. 2, pp 1–232. https://doi.org/10.1016/S1874-5679(06)80006-1.
(31) Saucedo-Espinosa, M. A.; Lapizco-Encinas, B. H. Exploiting Particle Mutual Interactions To Enable Challenging Dielectrophoretic Processes. *Anal. Chem.* **2017**, *89* (16), 8459–8467. https://doi.org/10.1021/acs.analchem.7b02008.
(32) Saucedo-Espinosa, M. A.; Lapizco-Encinas, B. H. Refinement of Current Monitoring Methodology for Electroosmotic Flow Assessment under Low Ionic Strength Conditions. *Biomicrofluidics* **2016**, *10* (3), 033104. https://doi.org/10.1063/1.4953183.
(33) O'Brien, R. W.; White, L. R. Electrophoretic Mobility of a Spherical Colloidal Particle. *J. Chem. Soc. Faraday Trans. 2 Mol. Chem. Phys.* **1978**, *74*, 1607–1626. https://doi.org/10.1039/F29787401607.
(34) Nakatuka, Y.; Yoshida, H.; Fukui, K.; Matuzawa, M. The Effect of Particle Size Distribution on Effective Zeta-Potential by Use of the Sedimentation Method. *Adv. Powder Technol.* **2015**, *26* (2), 650–656. https://doi.org/10.1016/j.apt.2015.01.017.
(35) Saville, D. A. Electrokinetic Effects. In *Van Nostrand's Scientific Encyclopedia*; John Wiley & Sons, Inc.: Hoboken, NJ, USA, 2005; pp 321–337. https://doi.org/10.1002/0471743984.vse2860.
(36) Dukhin, S. S.; Mishchuk, N. A. Intensification of Electrodialysis Based on Electroosmosis of the Second Kind. *J. Memb. Sci.* **1993**, *79* (2–3), 199–210. https://doi.org/10.1016/0376-7388(93)85116-E.
(37) Vaghef-koodehi, A.; Ernst, O. D.; Lapizco-Encinas, B. H. Separation of Cells and Microparticles in Insulator-Based Electrokinetic Systems. *Anal. Chem.* **2022**, *In Press.* https://doi.org/10.1021/acs.analchem.2c04366.
(38) Kumar, A.; Elele, E.; Yeksel, M.; Khusid, B.; Qiu, Z.; Acrivos, A. Measurements of the Fluid and Particle Mobilities in Strong Electric Fields. *Phys. Fluids* **2006**, *18* (12), 1–11. https://doi.org/10.1063/1.2397573.

For Table of Contents Only